Identifying the Electronic Character and Role of the Mn States in the Valence Band of (Ga,Mn)As

J. Fujii,[1] B. R. Salles,[1] M. Sperl,[2] S. Ueda,[3] M. Kobata,[3] K. Kobayashi,[3,4,5] Y. Yamashita,[3,6] P. Torelli,[1] M. Utz,[2] C. S. Fadley,[7,8] A. X. Gray,[7,8,9] J. Braun,[10] H. Ebert,[10] I. Di Marco,[11] O. Eriksson,[11] P. Thunström,[12] G. H. Fecher,[13] H. Stryhanyuk,[13] E. Ikenaga,[14] J. Minár,[10] C. H. Back,[2] G. van der Laan,[15] and G. Panaccione[1,*]

[1]*Istituto Officina dei Materiali (IOM)-CNR, Laboratorio TASC, in Area Science Park, S.S.14, Km 163.5, I-34149 Trieste, Italy*
[2]*Institut für Experimentelle Physik, Universität Regensburg, D-93040 Regensburg, Germany*
[3]*NIMS Beamline Station at SPring-8, National Institute for Materials Science, Sayo, Hyogo 679-5148, Japan*
[4]*Japan Atomic Energy Agency, Sayo, Hyogo 679-5148, Japan*
[5]*Hiroshima Synchrotron Radiation Center, Hiroshima University, 2-313 Kagamiyama, Higashi-Hiroshima 739-0046, Japan*
[6]*Advanced Electric Materials Center, National Institute for Materials Science, 1-1 Namiki, Tsukuba, Ibaraki 305-0044, Japan*
[7]*Department of Physics, University of California, Davis, Davis, California 95616, USA*
[8]*Material Sciences Division, Lawrence Berkeley National Laboratory, Berkeley, California 94720, USA*
[9]*Stanford Institute for Materials and Energy Sciences, SLAC National Accelerator Laboratory, Menlo Park, California 94025, USA*
[10]*Department of Chemistry, Ludwig Maximillian University, D-81377 Munich, Germany*
[11]*Department of Physics and Astronomy, Uppsala University, Box 516, SE-75120 Uppsala, Sweden*
[12]*Institute for Solid State Physics, Vienna University of Technology, 1040 Vienna, Austria*
[13]*Max Planck Institute for Chemical Physics of Solids, 01187 Dresden, Germany*
[14]*Japan Synchrotron Radiation Research Institute, SPring-8, Hyogo 679-5198, Japan*
[15]*Diamond Light Source, Chilton, Didcot, Oxfordshire OX11 0DE, United Kingdom*

(Received 4 June 2013; published 27 August 2013)

We report high-resolution hard x-ray photoemission spectroscopy results on (Ga,Mn)As films as a function of Mn doping. Supported by theoretical calculations we identify, for both low (1%) and high (13%) Mn doping values, the electronic character of the states near the top of the valence band. Magnetization and temperature-dependent core-level photoemission spectra reveal how the delocalized character of the Mn states enables the bulk ferromagnetic properties of (Ga,Mn)As.

DOI: 10.1103/PhysRevLett.111.097201 PACS numbers: 75.50.Pp, 73.20.−r, 79.60.−i, 85.75.−d

Understanding the electronic and magnetic properties of diluted magnetic semiconductors has been a major challenge in materials science over the last decade, and carrier-mediated ferromagnetism is undoubtedly one of the most discussed issues in diluted magnetic semiconductor research [1–6]. The case of the (Ga,Mn)As valence band is prototypical: Whether the states near the Fermi level, E_F, are best described in terms of dispersive states fully merged with the GaAs valence band or if these states preserve the character of an impurity band has been a subject of intense activity in solid-state science [3–6]. Both descriptions stand on experimental and theoretical arguments that favor one or the other vision [5–9], and more recently unified pictures have been presented [10–13]. Nonetheless, the crossover regime between impurity states at low doping and extended states at high doping, i.e., the essence of how ferromagnetism is established in (Ga,Mn)As, is far from a unified and clear description. Such a description is intimately linked to a further central question: how important is localization vs hybridization of carriers in the vicinity of E_F as a function of doping? Theoretical modeling has so far only offered an inconclusive contribution to this issue, since disorder and strong electronic correlations render realistic calculations difficult to perform. On the experimental front, full control of the system is hard to achieve and a limited number of direct measurements of the (GaMn)As valence band have been reported [14–18]. The need to overcome the solubility limit to obtain stable ferromagnetic order strongly influences the homogeneity of (Ga,Mn)As, thus producing e.g., a depletion zone near the interface accompanied by a strong reduction of the Curie temperature, T_C [19], and a profound difference between surface and bulk electronic properties [7,19].

In the present work, we exploit bulk-sensitive hard x-ray photoemission spectroscopy (HAXPES), corresponding to a severely suppressed ($<4\%$) surface contribution [20,21], where the combined measure of valence band and core level, including temperature-dependent core-level magnetic circular dichroism (MCD), allows a direct determination of the bulk density of states near E_F as a function of Mn doping. Supported by theoretical calculations, we observe that (i) a clear density of states (DOS) with Mn $3d$ character is present, starting at a Mn doping level as low as 1%, (ii) the Fermi energy is located well above the GaAs host valence band top, and (iii) the delocalized character of the Mn states has a direct link with the (Ga,Mn)As ferromagnetic properties.

We have studied three (Ga,Mn)As thin films (Mn 1%, 5%, and 13% doping, 18–50 nm of thickness). HAXPES measurements were carried out at SPring-8 (Japan) using linearly polarized x rays on beam line BL15XU and circularly polarized x rays on beam line BL47XU. The overall

energy resolution was set to 250 meV for core level and 150 meV for valence band experiments, as verified by measuring the Au valence band from a polycrystalline sample in thermal and electrical contact with the (Ga,Mn)As sample. Further details concerning the photoemission measurements, sample growth and characterization, and calculation methods can be found in Ref. [22].

In Fig. 1 we show successive images of the valence-band region of pure GaAs and Mn-doped samples, with increasing magnification of the near E_F zone. Experimental results [$h\nu = 5953$ eV, Figs. 1(a)–1(c)] are compared with the theoretical curves [Figs. 1(d)–1(f)] based on a one-step model of angle-integrated photoemission. For the sake of comparison, the GaAs spectra have been aligned to the (GaMn)As spectra using the binding energy (BE) position of the As 4s core level. The electronic structure calculations used for the one-step photoemission intensities are based on the fully self-consistent combination of density-functional theory, the coherent-potential approximation to describe the presence of the Mn dopant, and dynamical-mean-field theory (DMFT) as implemented within the multiple scattering Green's function formalism [23–27]. The self-energy is instead obtained by means of the exact diagonalization solver as in Ref. [12]. The calculations agree quantitatively with the experimental data over a wide BE range. The As 4s states are located at ~10 eV BE and their effective hybridization with the Mn 3d states is small as they are well separated in energy [Figs. 1(a)–1(d)]. Closer to E_F, the Mn 3d states of e_g symmetry hybridize weakly with a mixture of As 4p (mainly) and Ga 4p states. Instead, the Mn 3d states of t_{2g} symmetry exhibit a more significant hybridization just below E_F. In Fig. 1(c), high-resolution spectra measured in the vicinity of E_F are displayed for pure GaAs, 1% and 13% Mn doping. Also shown are the difference spectra, where the pure GaAs spectrum is subtracted from the 13% and 1% Mn spectra (orange and grey, respectively), in order to highlight the Mn contribution. In Fig. 1(f), the calculated difference spectra, GaAs subtracted from (GaMn)As, are presented for the local density approximation (LDA) and DMFT calculations (violet and green curves, respectively).

The spectral weight of the difference spectra in Fig. 1(c) is peaked at ~200 and ~250 meV below E_F for a Mn

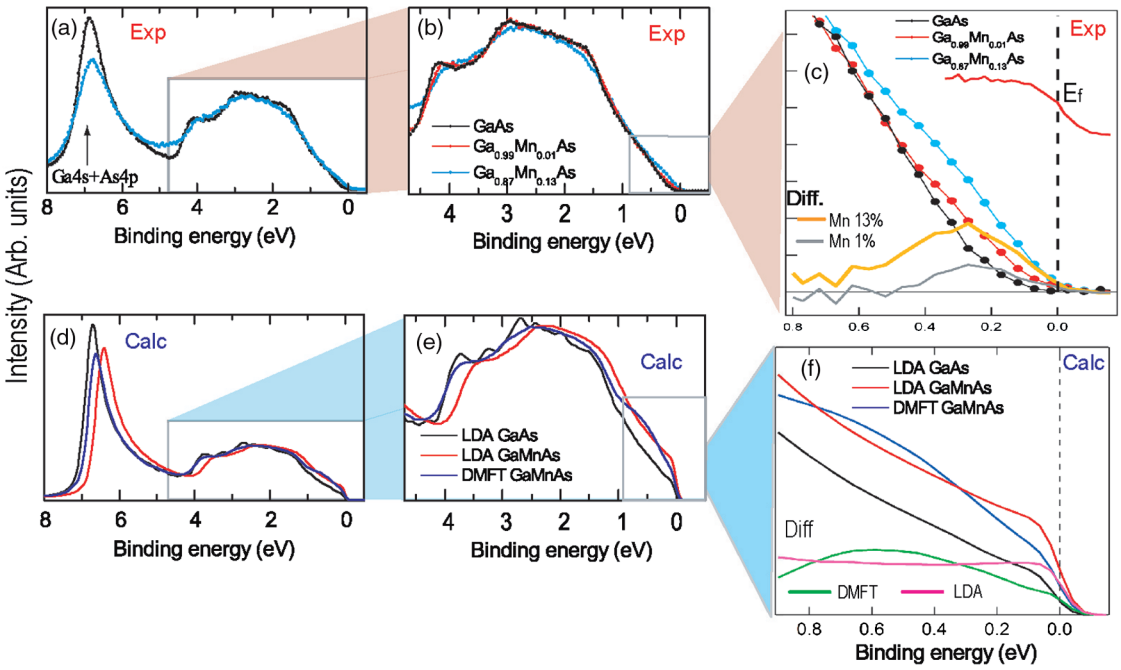

FIG. 1 (color online). (a)–(c) HAXPES spectra ($h\nu = 5953$ eV) for different Mn doping in GaAs. The GaAs spectra have been aligned to the (GaMn)As spectra using the BE position of the As 4s core level. No background subtraction was applied. (a) Extended valence band PES ($T = 20$ K), including the As 4s, Ga 4s, and As 4p shallow core levels of GaAs(100) and 13% Mn-doped GaAs. (b) Zoom of the valence band region ($T = 100$ K), showing the spectra from pure GaAs (black dots), 1% and 13% Mn-doped GaAs (red and blue dots, respectively). (c) High-resolution spectra measured in the vicinity of E_F. Difference spectra, corresponding to the Mn contribution only, are shown in orange [13% Mn spectrum (blue dots) minus pure GaAs spectrum (black dots)] and grey [1% Mn spectrum (red dots) minus pure GaAs spectrum (black dots)]. The reference Fermi level of Au is displayed, offset. (d) Calculated angle-integrated PES (including matrix elements) for photon energy and geometry (p polarization) as used in the experiment. (e) Calculated valence-band spectra of GaAs(100) using LDA (black curve) and (Ga,Mn)As (13%) using both LDA (red curve) and DMFT (blue curve). (f) Zoom of the vicinity of E_F with calculated difference spectra, as in (c), for LDA (violet curve) and DMFT (green curve).

content of 1% and 13%, respectively, in agreement with previous photoemission results [11,14,16]. The LDA calculation in Fig. 1(f), instead, exhibits a broad plateau, leading into poor agreement with experimental data. This agreement improves in LDA + DMFT, where a well-defined peak forms, but centered at ~500 meV. From the calculations we infer that the maximum in the difference signal has mainly a Mn-3d (t_{2g}) character. A strong hybridization is present with a mixture of mainly As 4p states localized around the impurity, and Mn 4p states. Therefore we identify the approximate treatment of this hybridization, which is inner to the exact diagonalization solver, as the main reason of the discrepancy in the peak position. It is important to emphasize that the Mn-related DOS near E_F, although significantly smaller, is nonzero within the energy resolution. The diluted nature of Mn in the host GaAs matrix is confirmed by the spectroscopic fingerprint of the difference spectra in Fig. 1(c): the Mn states in (Ga,Mn)As retain their Gaussian line shape (broadened when the doping value increases) up to a Mn doping as high as 13, whereas for MnAs, a truly metallic system, one obtains a clear Fermi edge [22].

Having ascertained the nature and evolution of the Mn states in the vicinity of E_F, we now use circularly polarized x rays (MCD-PES) to have access to magnetic information [28,29]. Figure 2 shows the core-level HAXPES ($h\nu$ = 7940 eV) for a 13% Mn-doped GaAs sample in the ferromagnetic state (below its Curie temperature, T_C = 80 K), and compared to model calculations. Figure 2(a) shows a survey spectrum that identifies the Mn 2p doublet with the well-screened and poorly screened features of the $2p_{3/2}$ and $2p_{1/2}$ core levels, in agreement with previous results [28,29]. Figure 2(b) shows the MCD for the full Mn 2p region, with a very large magnetic asymmetry of ~13%. The line shape of the Mn 2p core level does not change while varying the Mn concentration from 1% to 13%, which is strong evidence against an important contribution of interstitial Mn atoms in our bulk-sensitive spectra [28]. The calculations in Fig. 2(c), using the Anderson impurity model [22], shows that the $2p_{3/2}$ structure contains a well-screened peak at the high kinetic energy (low BE) side and a poorly screened peak at 1–2 eV lower kinetic energy (higher BE), with opposite dichroism [28,29]. The well-screened peak is found to have mainly $2p^5 3d^6 h^2$ character, while the poorly screened peak has mainly $2p^5 3d^5 h$ character, where h denotes a hole state. In the ground state, the $3d^5 h$ state is pinned to E_F, and it is the $3d^6 h^2$ state that is pulled down in energy in the final state due to the 2p core-hole potential [28]. In the calculation, the local ground state properties are primarily reflected by two parameters: The transfer integral V responsible for the hybridization (mixing) and the on-site 3d electron-repulsion energy U, i.e., the Hubbard U. The experimental MCD of the HAXPES agrees very well with the calculated spectra for a hybridization parameter 2.0 ≤ V ≤ 2.5 eV. The most

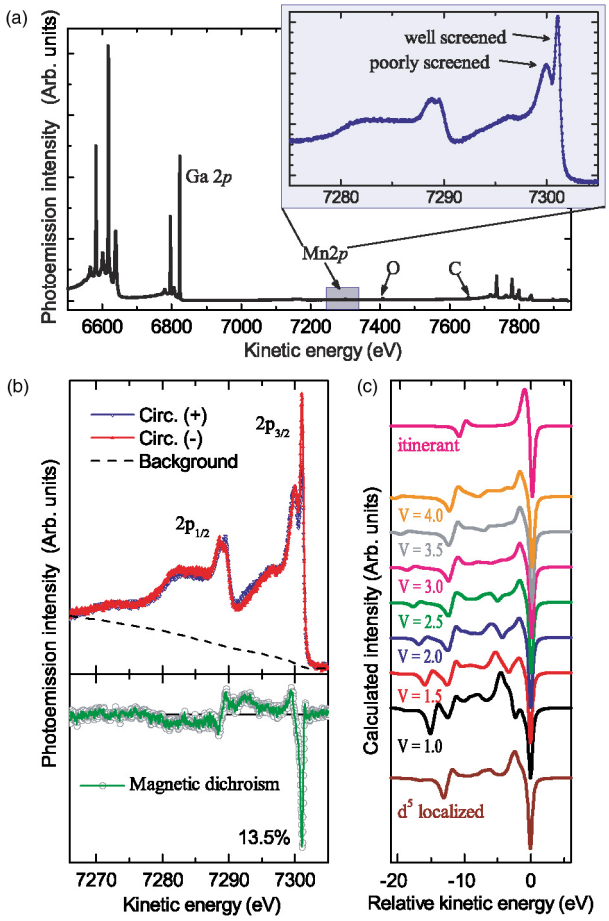

FIG. 2 (color online). (a) HAXPES wide energy scan ($h\nu$ = 7940 eV, linear polarization, T = 20 K) of 13% Mn-doped GaAs. Main lines positions are indicated. The inset shows a zoom of the Mn 2p core level with the $2p_{1/2}$ and $2p_{3/2}$ multiplet structure, where the well-screened and poorly screened peaks are indicated. For a definition of well-screened and poorly screened peaks in (GaMn)As see Ref. [25]. (b) MCD in HAXPES. Polarization-dependent Mn 2p spectra (blue and red dots for right- and left-circular polarization, respectively), measured at T = 20 K, i.e., below T_C; the dashed thin line represents the background. In the lower panel the difference spectrum (MCD), representing the magnetic signal (open white circles) is shown; the green line is a smoothed curve. The value of the maximum magnetic asymmetry, defined as $(I^+ - I^-)/(I^+ + I^-)$, where $I^+(I^-)$ is the intensity measured with Circ+ (Circ−), is indicated. (c) Calculations for an Anderson impurity model with varying hybridization V, as well as a fully localized d^5 state, and an itinerant electron model. The calculated curves are offset for clarity. The best agreement is for a hybridization parameter 2.0 ≤ V ≤ 2.5 eV.

intense magnetic signal, corresponding to the leading well-screened peak, is linked to the most delocalized electronic d character, an attribute already put forward by the results of Dobrowolska *et al.* [30] and in good agreement with Richardella *et al.* [13].

Additional evidence of the role played by the electron hybridization of the Mn 3d states is obtained from

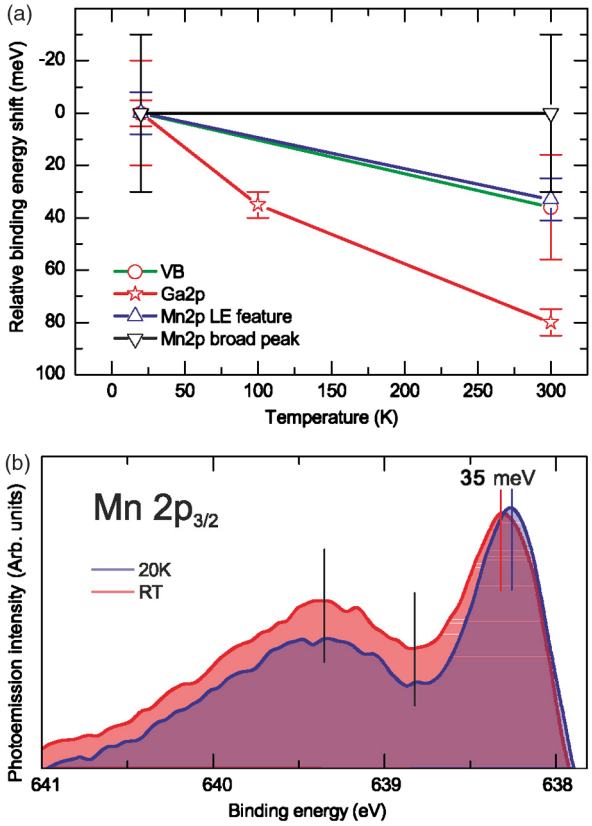

FIG. 3 (color online). Temperature dependence of the (Ga,Mn)As (13% Mn) PES. (a) Relative BE shift of the GaAs host valence band, Ga $2p$ core level, Mn $2p_{3/2}$ low energy feature, and Mn $2p_{3/2}$ broad peak; the BEs at 20 K are used as reference. (b) Mn $2p_{3/2}$ core level measured at 20 K and at RT.

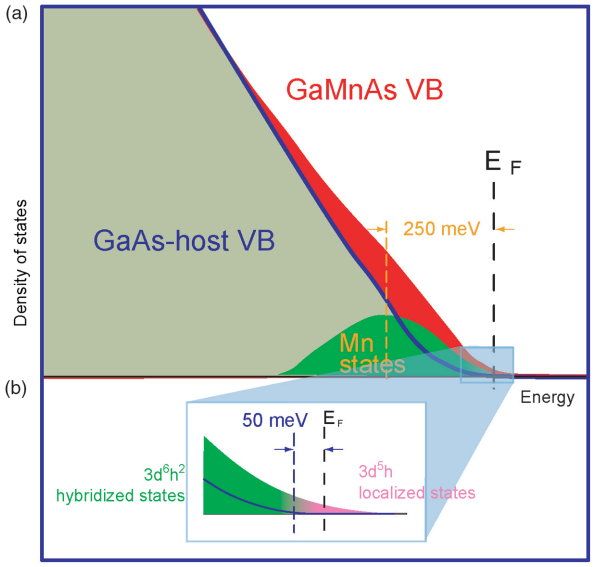

FIG. 4 (color online). Schematics of the electronic structure of (Ga,Mn)As. (a) Experimental valence band (smoothed) at $h\nu = 5953$ eV. GaAs host band (blue curve) and (Ga,Mn)As band with 13% Mn (red curve). The difference between both spectra identifies the Mn-derived states (dark green). The dashed vertical bar marks the position of E_F; the center of the Mn band is located at ~250 meV BE. (b) Zoom of the region near E_F. The GaAs host band does not cross E_F (energy separation of 50 meV); the Mn-induced states have a finite nonzero density at E_F. The color shading illustrates the difference in electronic character of the Mn d states as derived from our theoretical calculations: near E_F a $3d^5h$ localized character is found, whereas $3d^6h^2$ delocalized character is assigned to the dark green region. The latter corresponds to the hybridization responsible for mediating the ferromagnetism.

temperature-dependent HAXPES. Knowing that the carrier concentration in a heavily doped semiconductor, such as (GaMn)As, does not change significantly with temperature [30], a shift of the core levels and/or the valence band spectra vs temperature is associated with a change in the screening efficiency of the delocalized electrons. The HAXPES results are shown in Fig. 3 (13% Mn doping); while the Ga $2p$ peak shifts ~80 meV to higher BE between 20 K and room temperature, the measured valence-band shift is less than 40 meV. This temperature dependence implies an increased Mn $3d$-As $4p$ hybridization, and hence a more efficient hopping favoring ferromagnetism [28–32]. Moreover, the low BE feature of the Mn $2p_{3/2}$ core level (associated with the more delocalized d^6h^2 states) shifts with temperature by ~35 meV, whereas no shift of the broad component at higher BE (corresponding to the more localized d^5h states) is detected. This observation confirms that the screening is associated exclusively to the more hybridized Mn $3d$ states, d^6h^2, while the localized d^5h states, near E_F, do not participate in the screening process. A further confirmation of this picture comes from the calculated MCD-PES in Fig. 2(b), where the energy separation between the sharp negative peak and broad positive peak in the Mn $2p_{3/2}$ increases with V; this again implies a more efficient screening due to delocalized electrons.

The physical scenario emerging from our combined observations and calculations is presented in Fig. 4. The GaAs valence band is substantially modified by the introduction of Mn atoms, even for doping values as low as 1%. The largest modification of the GaAs host band is found over 2–4 eV BE. The energy separation from the top of the GaAs-host states to E_F is in the order of 50 meV, after taking into account the experimental energy resolution, convolution with the Fermi function, and possible recoil effects [22]. We note that in a real impurity system, i.e., when disorder is included, Bloch states are never formed and the concept of delocalized states in the Mn-derived band with a clear E vs k relation cannot be fully defined. Thus the term "band" does not imply electronic states of well-defined crystal momentum, while the DOS remains a well-defined quantity. In the present case, angle-integrated HAXPES measures only the DOS: because of the high photon energy used ($h\nu \geq 5$ keV), band structure effects can be neglected [21].

In conclusion, the present experimental observations of a persistent diluted character of Mn in GaAs, together with E_F located well above the GaAs valence band top, as found by Ohya *et al.* [8], suggest that the existence of a Mn-derived band which is not detached from the GaAs bands, could be compatible at the same time with localization (impurity band) character.

Two of us (A. X. G. and C. S. F.) gratefully acknowledge the support of the U.S. Department of Energy under Contract No. DE-AC02-05CH11231. Financial support from the German funding agencies DFG (FOR 1346, SFB 689, EB 154/23 and 18), the German ministry BMBF (05K10WMA), and the Austrian Science Fund (FWF project ID I597-N16) is also gratefully acknowledged (J. M., J. B., H. E., and P. T.). I. D. M. and O. E. are grateful to the Swedish Research Council (VR), Energimyndigheten (STEM), the KAW Foundation, and ERC (247062-ASD). We like to thank M. I. Katsnelson for useful discussions.

*panaccioneg@elettra.trieste.it

[1] A. H. MacDonald, P. Schiffer, and N. Samarth, Nat. Mater. **4**, 195 (2005).
[2] I. Žutić, J. Fabian, and S. Das Sarma, Rev. Mod. Phys. **76**, 323 (2004).
[3] C. Chappert, A. Fert, and F. N. Van Dau, Nat. Mater. **6**, 813 (2007).
[4] N. Samarth, Nat. Mater. **11**, 360 (2012).
[5] T. Dietl, Nat. Mater. **9**, 965 (2010).
[6] T. Jungwirth, J. Sinova, J. Mašek, J. Kučera, and A. H. MacDonald, Rev. Mod. Phys. **78**, 809 (2006).
[7] T. Dietl, H. Ohno, F. Matsukura, J. Cibert, and D. Ferrand, Science **287**, 1019 (2000).
[8] S. Ohya, K. Takata, and M. Tanaka, Nat. Phys. **7**, 342 (2011); I. Muneta *et al.*, arXiv:1208.0575.
[9] J. Mašek *et al.*, Phys. Rev. Lett. **105**, 227202 (2010).
[10] K. Sato *et al.*, Rev. Mod. Phys. **82**, 1633 (2010).
[11] A. X. Gray *et al.*, Nat. Mater. **11**, 957 (2012).
[12] I. Di Marco *et al.*, arXiv:1207.2887v1.
[13] A. Richardella, P. Roushan, S. Mack, B. Zhou, D. A. Huse, D. D. Awschalom, and A. Yazdani, Science **327**, 665 (2010).
[14] J. Okabayashi, A. Kimura, O. Rader, T. Mizokawa, A. Fujimori, T. Hayashi, and M. Tanaka, Phys. Rev. B **64**, 125304 (2001).
[15] J. Okabayashi, A. Kimura, O. Rader, T. Mizokawa, A. Fujimori, T. Hayashi, and M. Tanaka, Phys. Rev. B **58**, R4211 (1998).
[16] M. Kobayashi *et al.*, arXiv:1302.0063.
[17] O. Rader *et al.*, Phys. Rev. B **69**, 075202 (2004).
[18] H. Åsklund, L. Ilver, J. Kanski, J. Sadowski, and R. Mathieu, Phys. Rev. B **66**, 115319 (2002).
[19] M. Sawicki, D. Chiba, A. Korbecka, Y. Nishitani, J. A. Majewski, F. Matsukura, T. Dietl, and H. Ohno, Nat. Phys. **6**, 22 (2010).
[20] G. Panaccione and K. Kobayashi, Surf. Sci. **606**, 125 (2012).
[21] A. X. Gray *et al.*, Nat. Mater. **10**, 759 (2011).
[22] See Supplemental Material at http://link.aps.org/supplemental/10.1103/PhysRevLett.111.097201 for detailed information concerning the sample preparation, the magnetic and electronic characterization, and the details of calculations.
[23] J. Minár, J. Phys. Condens. Matter **23**, 253201 (2011).
[24] H. Ebert, D. Ködderitzsch, and J. Minár, Rep. Prog. Phys. **74**, 096501 (2011).
[25] P. Thunström, I. DiMarco, and O. Eriksson, Phys. Rev. Lett. **109**, 186401 (2012).
[26] G. Kotliar, S. Savrasov, K. Haule, V. Oudovenko, O. Parcollet, and C. Marianetti, Rev. Mod. Phys. **78**, 865 (2006).
[27] J. Braun, J. Minár, F. Matthes, C. M. Schneider, and H. Ebert, Phys. Rev. B **82**, 024411 (2010).
[28] J. Fujii *et al.*, Phys. Rev. Lett. **107**, 187203 (2011).
[29] K. W. Edmonds, G. van der Laan, N. R. S. Farley, R. P. Campion, B. L. Gallagher, C. T. Foxon, B. C. C. Cowie, S. Warren, and T. K. Johal, Phys. Rev. Lett. **107**, 197601 (2011).
[30] M. Dobrowolska, K. Tivakornsasithorn, X. Liu, J. K. Furdyna, M. Berciu, K. M. Yu, and W. Walukiewicz, Nat. Mater. **11**, 444 (2012).
[31] S. Kim, C.-S. Son, S. W. Chung, Y. K. Park, E. K. Kim, and S.-K. Min, Thin Solid Films **310**, 63 (1997).
[32] G. Van der Laan, K. W. Edmonds, E. Arenholz, N. R. S. Farley, and B. L. Gallagher, Phys. Rev. B **81**, 214422 (2010).